Chemical Science

Accepted Manuscript

Chemical Science

rsc.li/chemical-science

Volume 9
Number 1
7 January 2018
Pages 1-268

ISSN 2041-6539

ROYAL SOCIETY OF CHEMISTRY

EDGE ARTICLE
Xinjing Tang et al.
Caged circular siRNAs for photomodulation of gene
expression in cells and mice

This is an Accepted Manuscript, which has been through the Royal Society of Chemistry peer review process and has been accepted for publication.

Accepted Manuscripts are published online shortly after acceptance, before technical editing, formatting and proof reading. Using this free service, authors can make their results available to the community, in citable form, before we publish the edited article. We will replace this Accepted Manuscript with the edited and formatted Advance Article as soon as it is available.

You can find more information about Accepted Manuscripts in the Information for Authors.

Please note that technical editing may introduce minor changes to the text and/or graphics, which may alter content. The journal's standard Terms & Conditions and the Ethical guidelines still apply. In no event shall the Royal Society of Chemistry be held responsible for any errors or omissions in this Accepted Manuscript or any consequences arising from the use of any information it contains.

ROYAL SOCIETY OF CHEMISTRY

rsc.li/chemical-science

EDGE ARTICLE

Unlocking Radical Reactivity of Cyclic Diaryl λ³-Chloranes Through NHC-Catalyzed Three-Component Coupling

Anusree A. Kunhiraman[a], Koushik Patra[a], Venkata Surya Kumar Choutipalli[b], Manjeet Godara[a], Kevin L. Shuford*[b] and Mahiuddin Baidya*[a]

Hypervalent halogens are central to contemporary organic synthesis, yet hypervalent chloranes, particularly cyclic λ³-chloranes, remain markedly underexplored, despite their unique electronic properties imparted by the highly electronegative chlorine atom. To date, their radical reactivity has not been documented. Herein, we report the first radical reaction of cyclic diaryl λ³-chloranes, enabled by N-heterocyclic carbene (NHC) catalysis in a three-component reaction with aromatic aldehydes and olefins at room temperature. This strategy leverages the strong reducing power of the NHC-derived Breslow enolate to generate a biaryl radical from the λ³-chlorane, initiating a radical relay that culminates in regioselective vicinal aroylarylation of olefins. This transition-metal-free methodology provides streamlined access to ortho-substituted unsymmetrical biaryls in high yields, with broad functional group tolerance and compatibility with biorelevant scaffolds. Mechanistic insights from DFT calculations reveal that the key single-electron transfer (SET) from the Breslow enolate to the λ³-chlorane is a barrierless process, markedly distinct from the analogous λ³-bromane and λ³-iodane species. The favorable kinetics of the radical relay event and the thermodynamic stability of the aroylarylated products drive the reaction selectively along the desired three-component pathway.

Introduction

The chemistry of hypervalent halogens has become a cornerstone in modern organic synthesis, offering innovative pathways for creating complex molecules under mild conditions.[1] Their unique electronic structure and properties, coupled with low toxicity, contribute to distinct reactivity that often complements the mechanistic rationale of transition metal catalysis, amplifying their relevance in chemical science.[1,2] Over the years, major advancements in this field have largely been driven by the development of λ³-iodanes and λ³-bromanes.[2,3] Surprisingly, ascending of their isoelectronic congener, λ³-chloranes, remains immature, albeit they could exhibit increased reactivity owing to the higher electronegativity and ionization potential of chlorine compared to iodine and bromine.[4] Breakthrough came recently with the introduction of cyclic diaryl λ³-chloranes (1) from Wencel–Delord group (Scheme 1a).[5] They have manifested the elevated nucleofugality property of 1 leading to the formation of benzyne intermediate under basic conditions, which was then trapped by nucleophiles to expedite steric-effect governed preferential meta-functionalization (Scheme 1a). Our research group also leveraged nucleophile capture reactivity of 1 and disclosed the highly ortho-selective ligand coupling reactivity under metal-free conditions (Scheme 1a).[6] However, these methodologies primarily reflect polar chemistry, the classical two-electron reaction pathway

of λ³-chlorane (1). At this juncture, the one-electron reaction pathway, the so-called radical reaction modality, of 1 under metal-free conditions remains largely unexplored. Meanwhile, the thermal rearrangement of μ-sulfoxo diaryl cyclic λ³-chloranes to homodimerized biaryls was recently observed by Wirth group, where a radical reaction pathway was proposed.[7] Obviously, the successful realization of radical reactivity in versatile cyclic diaryl λ³-chloranes (1) beyond classical polar mechanism, particularly in a multicomponent fashion, holds the potential to open new avenues in contemporary organic synthesis.

The persistent ketyl radicals have a rich history.[8] Recently, they have been judiciously integrated within the N-heterocyclic carbene (NHC) catalysis to harness NHC radical catalysis.[9] This reactivity takes advantage of the strong reducing power of the Breslow enolate intermediate, which undergoes single electron transfer (SET) to generate the persistent ketyl radical for subsequent functionalization (Scheme 1b).[9,10] In this context, the pioneering contribution from Ohmiya group on the decarboxylative coupling of aryl aldehydes and redox-active esters to produce sterically congested ketone[11l] and further advancements by others are highly intriguing.[11] We question whether cyclic diaryl λ³-chloranes could be engaged as SET reagent in NHC radical catalysis to access biaryl radicals, which is so far elusive. We envisioned a three-component coupling involving λ³-chlorane (1), aldehyde (2), and alkene (3) (Scheme 1c). Strategically, the enolate form of the Breslow intermediate A1, generating through the reaction of aldehyde (2) with NHC, could potentially affect SET to the cyclic diaryl λ³-chlorane (1), exploiting the oxidizing power of λ³-chlorane and rapid carbon–chlorine bond cleavage to generate the pivotal biaryl radical A2 and NHC-bound ketyl-radical A3 (Scheme 1c). Then, they induce a radical relay process with alkene (3) to give intermediate A4, which would subsequently break down to release
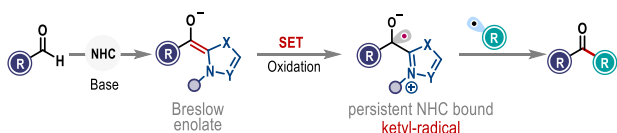
a. Department of Chemistry, Indian Institute of Technology Madras, Chennai 600036, India, Email: mbaidya@iitm.ac.in.

b. Department of Chemistry and Biochemistry, Baylor University, One Bear Place #97348, Waco, Texas 76798-7348, United States.

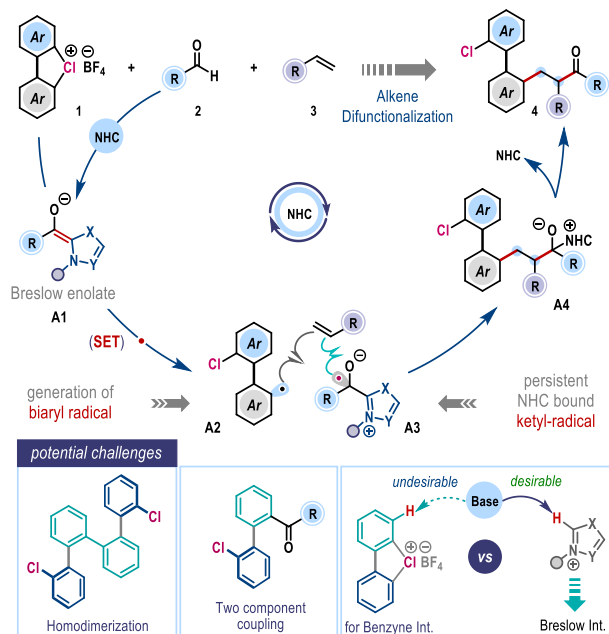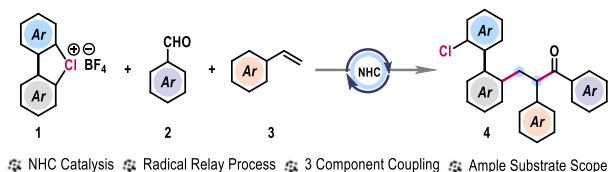†Electronic supplementary information (ESI) available.
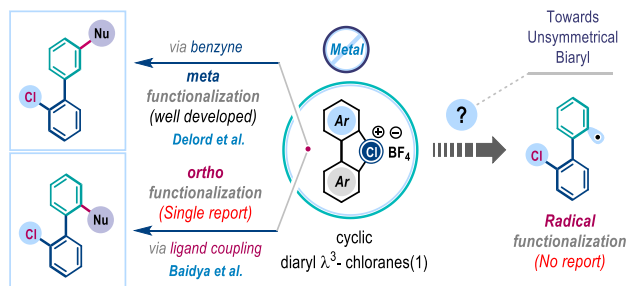
Scheme 1: Cyclic diaryl λ³-chloranes and NHC radical catalysis

biaryl-embedded alkene difunctionalization product **4** with the regeneration of NHC catalyst (Scheme 1c). However, significant challenges persist in mitigating the formation of homo-coupling[7] and two-component byproducts, as well as in controlling regioselectivity. Furthermore, NHC catalysis operates under basic conditions that inherently favor the benzyne pathway[5], as discussed in the preceding section, which must be effectively suppressed to unlock the desired radical reactivity of λ³-chloranes (Scheme 1c, below).

Herein, we report the development of this approach and delineate the first example of the radical reactivity of cyclic diaryl λ³-chloranes through *N*-heterocyclic carbene (NHC) catalysis (Scheme 1d). This methodology capitalizes on the metal-free coupling of cyclic diaryl λ³-chloranes, aldehydes, and alkenes to offer a wide range of functionally enriched unsymmetrically *ortho*-disubstituted biaryls in high yields at room temperature. In a nutshell, it regioselectively installs an aroyl group and a biaryl unit across the olefin functionality in a single operation. This catalytic aroylarylation protocol is operationally simple, scalable, and applicable to a wide variety of substrates, including those relevant to pharmaceuticals and materials. DFT calculations were also performed to elucidate the intricacy in the reaction mechanism.

Result and Discussion

Table 1. Optimization of reaction conditions[a,b,c]
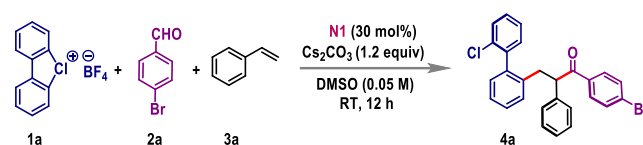
Entry	Deviation from the standard conditions	Yield of **4a** (%)[b,c]
1	DCE / CH₃CN / TFT instead of DMSO	NR
2	1,4-Dioxane / DCM instead of DMSO	NR
3	DMF instead of DMSO	32
4	**None**	**86**
5	with **N2 / N3** instead of **N1**	41 / NR
6	KOᵗBu / Na₂CO₃ / K₂CO₃ instead of Cs₂CO₃	NR / 63 / 70
7	Et₃N/ DMAP instead of Cs₂CO₃	34 / NR
8	1.0 / 2.0 equiv of **1a** instead of 1.5 equiv	50 / 67
9	1.5 / 3.0 equiv of **3a** instead of 2.0 equiv	72 / 80
10	with 20 mol% of **N1**	62
11	without **N1**	NR
12	with **1-N₂BF₄** instead of **1a**	NR

NHC Catalysts
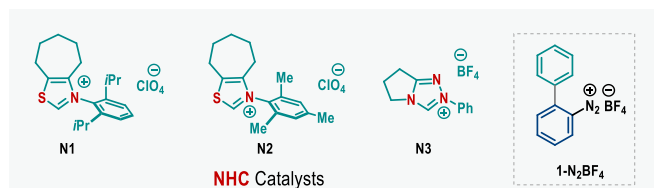
[a]Reaction conditions: **1a** (0.3 mmol), **2a** (0.2 mmol), **3a** (0.4 mmol), Cs₂CO₃ (1.2 equiv), NHC (0.06 mmol) and solvent (4.0 mL), 12 h. [b]Isolated yields are given. [c]In all cases, 1:1 *dr* was obtained. NR: No reaction.

Our investigations began following the three-component coupling of cyclic diaryl λ³-chlorane **1a**, 4-bromobenzaldehyde **2a**, and styrene **3a** as a model reaction (Table 1). Initially, we screened various solvents using thiazolium salt **N1** as the NHC precursor in the presence of Cs₂CO₃ base (entries 1, 2). However, most solvents were ineffective, leading primarily to the decomposition of λ³-chlorane **1a**. A breakthrough was achieved when the reaction was conducted in

DMF, which produced **4a**, albeit in a modest 32% yield (entry 3). Notably, when DMSO was used as the solvent, the reaction proceeded cleanly, offering the desired product **4a** in 86% isolated yield (entry 4). Employment of other thiazolium salts revealed a moderate reactivity for **N2**, while the reaction was unfruitful with the triazolium-based NHC precursor **N3** (entry 5). Examination of other inorganic bases showed that KO^{t}Bu was ineffective; however, K$_2$CO$_3$ and Na$_2$CO$_3$ promote this reaction, giving **4a** in 70% and 63% yields, respectively (entry 6). Detrimental outcomes were also obtained for organic bases such as Et$_3$N or DMAP (entry 7). The loading of reaction components was crucial for achieving high yields. Variations in the amounts of **1a** or **3a** resulted in suboptimal outcomes (entries 8-9).

Additionally, reducing the catalyst loading to 20 mol% lowered the yield to 62%, and the reaction completely failed in the absence of the NHC catalyst (entries 10-11). Also, this NHC catalyzed SET process was not effective with the biaryl diazonium precursor **1-N$_2$BF$_4$**, indicating the significance of cyclic diaryl λ^3-chlorane for this coupling reaction (entry 12).

After identifying the optimized reaction conditions (Table 1, entry 4), we turned our attention to exploring the scope of the three-component radical coupling reaction (Scheme 2). First, the influence

Scheme 2: Exploration of substrate scope^{a,b,c}
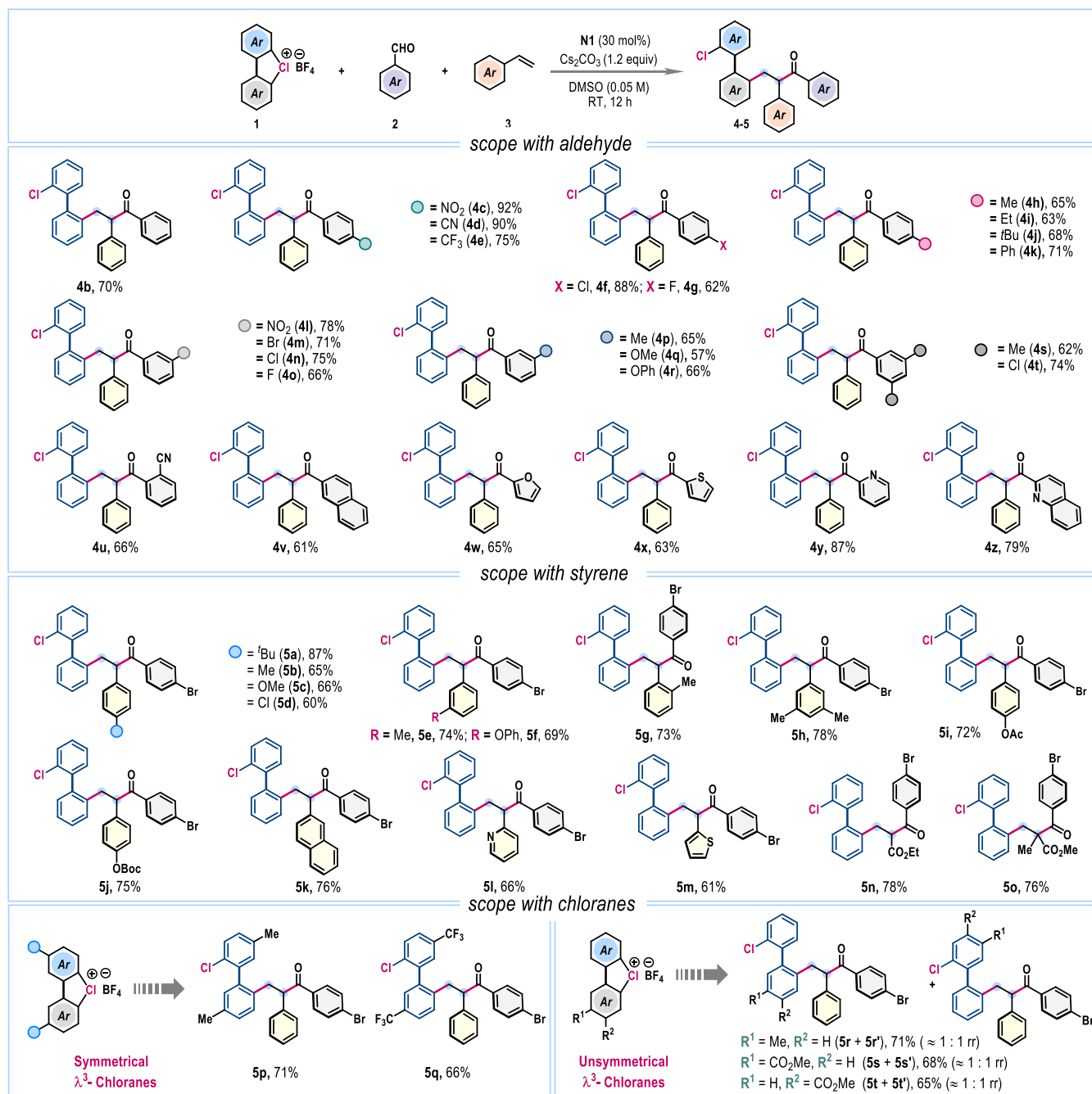
^{a}Reaction conditions: **1** (0.3 mmol), **2** (0.2 mmol), **3** (0.4 mmol), **N1** (30 mol%), Cs$_2$CO$_3$ (1.2 equiv), and DMSO (4.0 mL), rt, 12 h. ^{b}Isolated yields are provided. ^{c}≈1:1 *dr* was obtained for all cases.

of substitutions in aldehyde (**2**) was evaluated. Satisfyingly, along with parent benzaldehyde (**4b**), a wide range of aromatic aldehydes bearing electron-withdrawing nitro (**4c**), cyano (**4d**), trifluoromethyl (**4e**), and halogen (**4f**, **4g**) functionalities and electron-donating alkyl (**4h**–**4j**) and phenyl (**4k**) groups at the *para*-position of the arene ring effectively participated, dispensing functionally enriched unsymmetrical 2,2′-disubstituted biphenyls in good to very high yields. Similarly, *meta*-substituted aromatic aldehydes smoothly furnished desired products **4l**–**4t** in good yields. Sterically hindered *ortho*-substitution (**4u**) and bulky β-naphthaldehyde (**4v**) were also amenable. Importantly, aldehydes bearing heteroaromatic scaffolds such as furan (**4w**), thiophene (**4x**), pyridine (**4y**), and quinoline (**4z**) did not hamper the reaction, affording corresponding products in 63%–87% yields (Scheme 2). However, examination of aliphatic aldehydes under the standard reaction conditions was unsuccessful (ESI, Page S5).

Next, the compatibility of the styrene coupling partner (**3**) was examined, which also proved quite general (Scheme 2). Styrenes with alkyl, alkoxy, aryloxy, and halogen functionalities at various positions in the phenyl unit were suitable, forming desired products **5a**–**5h** in 60%–87% yields. Common protecting groups such as acetyl and *tert*-butyloxycarbonyl (Boc) were also undisturbed to give **5i** and **5j** in 72% and 75% yields, respectively. Also, 2-vinylnaphthalene (**5k**), 2-vinylpyridine (**5l**), and 2-vinylthiophene (**5m**) were amenable to afford good yields. Significantly, three-component coupling was effective with electron-deficient alkenyl esters, for example, ethyl acrylate and methyl methacrylate, producing **5n** and **5o** in 78% and 76% yields, respectively (Scheme 2).

Further, we explored the effect of different substitutions on cyclic diaryl λ³-chloranes (**1**). Symmetrically substituted λ³-chloranes, bearing electron-donating methyl and electron-withdrawing trifluoromethyl groups, gave unsymmetrical biaryls **5p** and **5q** in 71% and 66% yields, respectively (Scheme 2). When unsymmetrically substituted cyclic diaryl λ³-chloranes were employed, an inseparable mixture of regioisomers was obtained, attributed to radical functionalization occurring at both aromatic rings of the unsymmetrical λ³-chloranes (Scheme 2). A nearly 1:1 ratio of regioisomeric products was observed for substrates bearing either electron-donating (**5r** and **5r′**) or electron-withdrawing (**5s** and **5s′**; **5t** and **5t′**) substituents, suggesting that electronic effects play only a minor role in this radical functionalization process. Notably, this outcome contrasts sharply with our previous findings in ligand-coupling reactions, where functionalization preferentially occurred at the electron-deficient arene ring of unsymmetrical λ³-chloranes.[6]

To further augment the versatility of this NHC-catalyzed three-component radical coupling protocol, we considered the difunctionalization of acenaphthylene, a renowned scaffold in material science.[12] Gratifyingly, under the standard reaction conditions, the coupling of λ³-chlorane **1a**, 4-bromobenzaldehyde **2a**, and acenaphthylene **6a** proceeded effectively to furnish the desired difunctionalized 1,2-dihydroacenaphthylene **7a** in 71% yield (Scheme 3). We were pleased to observe exclusive *trans*-selectivity for the

two newly installed functionalities. The protocol exhibited success across a range of aromatic and heteroaromatic aldehydes, facilitating the creation of a concise library of valuable 1,2-dihydroacenaphthylenes **7b**–**7i**, generally obtained in good yields (Scheme 3). The compound **7h** was crystalized and the single crystal X-ray analysis unambiguously confirmed both the product's structure and its stereochemistry. The reaction conditions were also effective for the difunctionalization of indene, successfully producing **7j** in synthetically useful yield without compromising *trans*-selectivity (Scheme 3).

**Scheme 3.** Towards difunctionalization of acenaphthylene and indene[a]
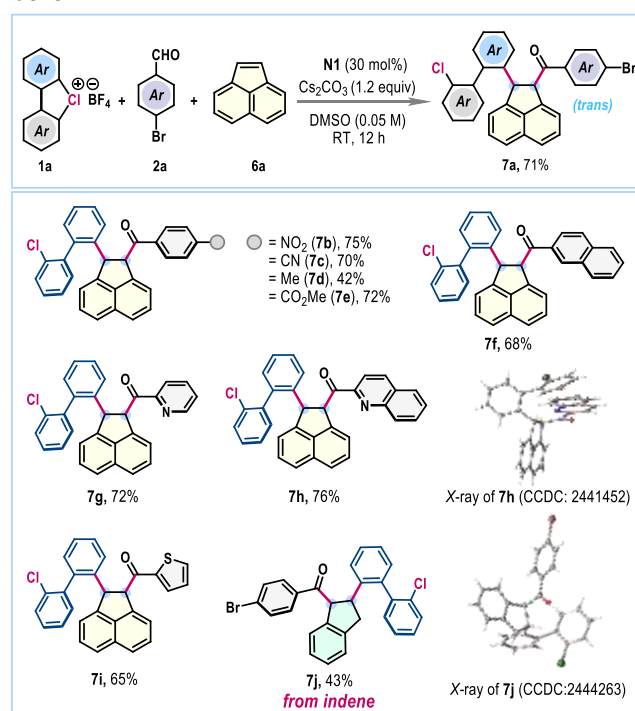
[a]Reaction conditions: **1a** (0.3 mmol), **2a** (0.2 mmol), **6a** (0.4 mmol), **N1** (30 mol%), Cs₂CO₃ (1.2 equiv), and DMSO (0.05 M), rt, 12 h. Isolated yields are provided and in all cases ≈1:1 *dr* was obtained.

To underscore the broad applicability and accommodate increased structural complexity within this three-component radical functionalization, substrates featuring biologically relevant scaffolds were investigated (Scheme 4). Notably, aldehydes derived from diverse bioactive frameworks, such as thymol (**8a**), (*L*)-menthol (**8b**), β-citronellol (**8c**), umbelliferone (**8d**), and diacetone-D-galactose (**8e**), underwent the transformation smoothly, affording the desired functionally enriched products in good yields. Likewise, styrenes bearing pharmacologically relevant motifs, including those derived from ibuprofen and clofibric acid, furnished products **8f** and **8g** in 53% and 51% yields, respectively (Scheme 4). With acenaphthylene, the aldehyde derived from thymol gave the desired product **8h** in 45% yield (Scheme 4).

ARTICLE

Scheme 4. Three-component radical coupling with biorelevant scaffolds.[a]
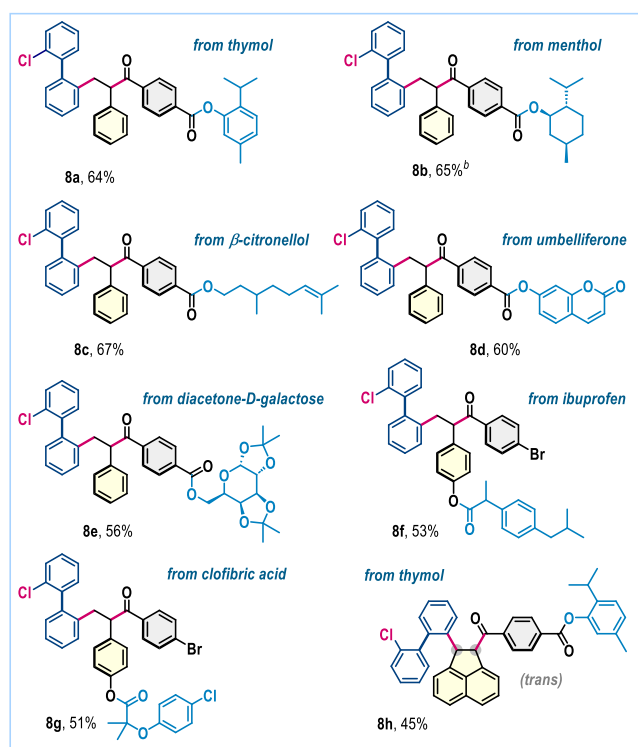
[a]Reaction conditions: as in Scheme 2. Isolated yields are provided and ≈1:1 dr was obtained. [b]For **8b** a dr of 1:1:1:1 was obtained.

Scheme 5. Scale-up reactions and post-synthetic applications.
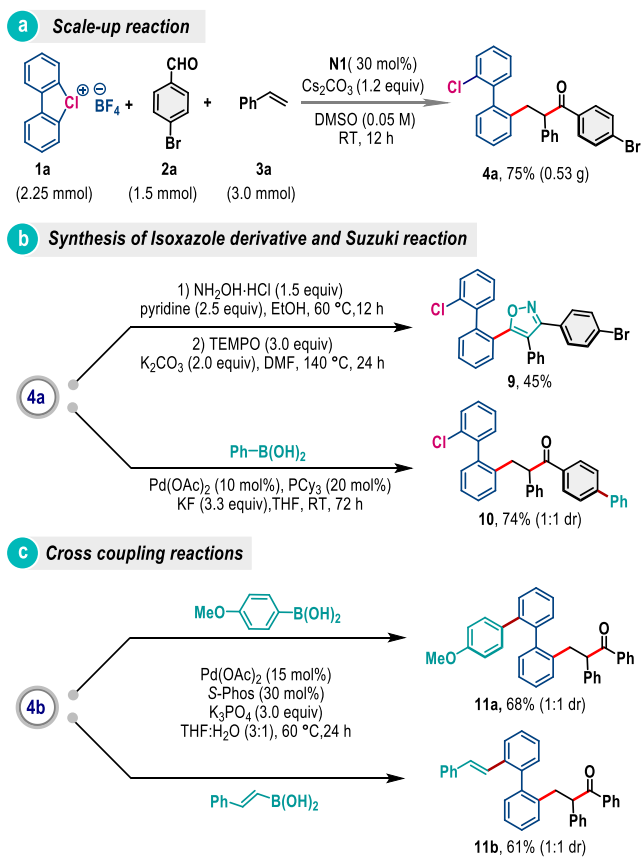
To demonstrate the synthetic utility, we have carried out scale-up reaction and product **4a** was obtained in 75% yield from 1.5 mmol scale reaction (Scheme 5a). The product **4a** was also transformed into isoxazole embedded biaryl **9** by treating with hydroxylamine followed by TEMPO mediated cyclization reaction (Scheme 5b).[13] Further diversification has been accomplished through site-selective Suzuki coupling, offering biaryl **10** in 74% yield (Scheme 5b). Similarly, product **4b** was exposed to palladium-catalyzed carbon-carbon coupling reaction conditions with 4-methoxyphenylboronic acid and trans-2-phenylvinylboronic acid, where products **11a** and **11b** were formed in 68% and 61% yields, respectively (Scheme 5c).

To provide insight into the mechanism, few control experiments were conducted. The reaction was significantly suppressed in the presence of radical scavengers such as TEMPO and BHT, suggesting the formation of a radical species (Scheme 6a). Additionally, we detected the TEMPO adduct **12** through HRMS, further supporting the formation of biaryl radical. The reactivities of cyclic diaryl λ³-chlorane (**1a**), λ³-bromane (**1a'**) and λ³-iodane (**1a''**) were compared (Scheme 6b). Under the standard reaction conditions, **1a'** gave the three-component coupling product **4a'**, albeit in significantly lower yield. In contrast, product formation was negligible for λ³-iodane (**1a''**). The superior reactivity of cyclic diaryl λ³-chlorane can be attributed to the higher electronegativity of chlorine compared to bromine and iodine, which leads to faster bond dissociation.

To gain deeper insights into the reaction mechanism, density functional theory (DFT) calculations were performed (Scheme 6c). The process initiates with a nucleophilic attack by the carbene species **A** on aldehyde **2a**, forming a tetrahedral intermediate **B** via the transition state **TS1** (13.36 kcal/mol). Subsequent base-mediated deprotonation leads to the formation of intermediate **C** (-30.12 kcal/mol), commonly referred to as Breslow enolate, in a highly exergonic step. To examine the SET hypothesis, we constructed a combined system of **C** and **1a**, mimicking the proposed experimental conditions. Upon geometry optimization, the system spontaneously evolved via C–Cl bond cleavage in the **1a** unit, generating two neutral radicals **D** and **1a•**. This transformation is exergonic by -41.44 kcal/mol (-71.56 kcal/mol, Scheme 6c), reinforcing the feasibility of the SET-driven bond activation. Analogous calculations for the bromonium and iodonium congeners of **1a** revealed similarly exothermic transformations, though to a lesser extent, with computed reaction energies of -17.51 kcal/mol and -7.76 kcal/mol, respectively (Scheme 6c). A closer examination of the optimized geometries of the resulting radical species reveals notable differences in structural distortion at the biphenyl moiety. Specifically, the dihedral angle in the bromonium (**1a'•**) and chloronium radicals (**1a•**) are significantly more distorted, at 25.27° and 37.88°, respectively.Whereas, the radical species formed from λ³-iodane remains nearly planar at 0.01°(Figure 1). The minimal structural perturbation and relatively modest reaction energy associated with the formation of iodonium radical suggest that this species may be susceptible to a thermodynamically favorable back electron transfer reaction under realistic conditions.

Scheme 6. Mechanistic investigation.[a]
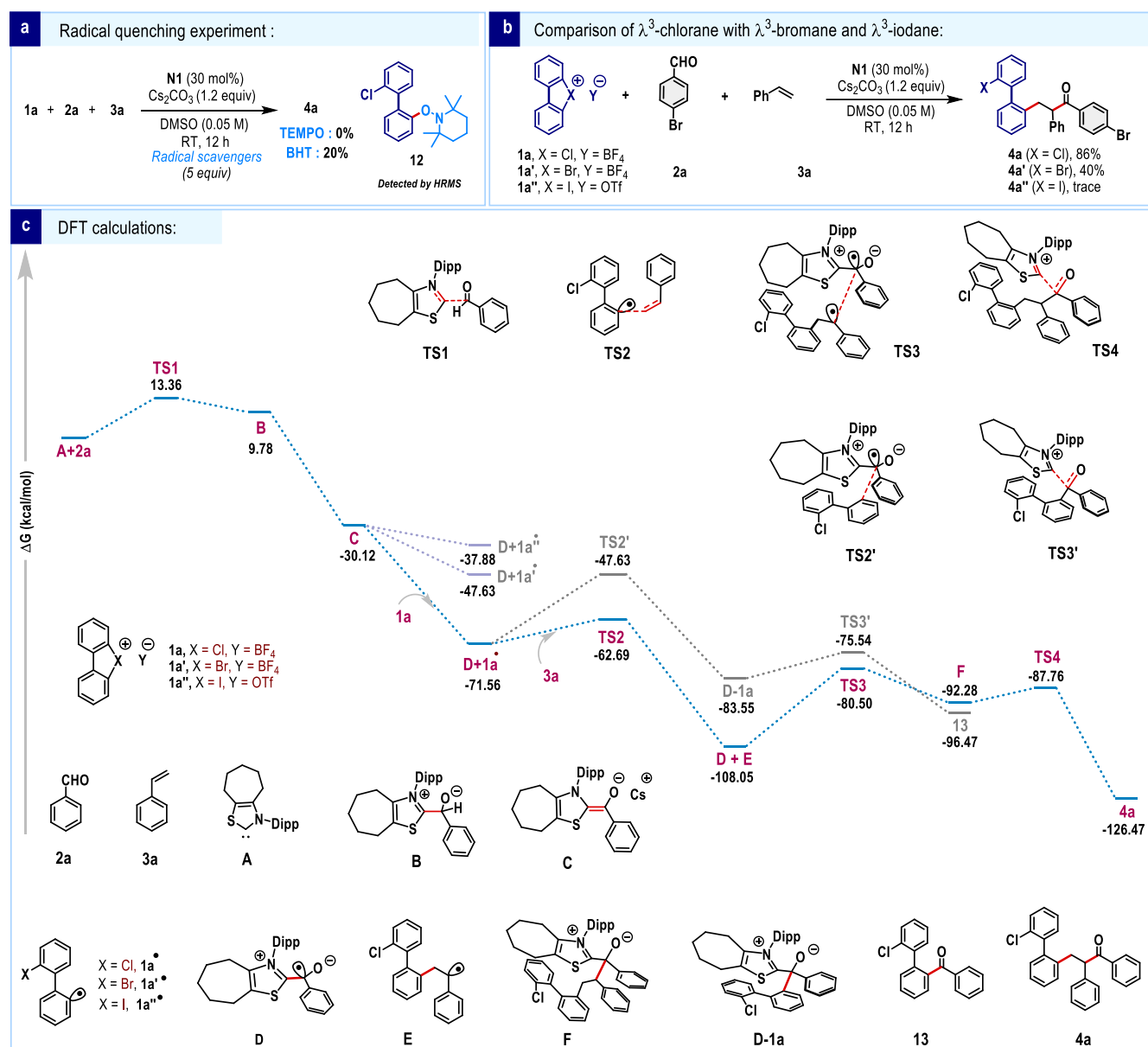
[a]All DFT calculations were performed using Gaussian 16 (Rev. C.01) with the ωB97X-D functional and def2-TZVP basis set. Geometries were optimized, and vibrational frequency and IRC analyses were used to confirm minima and transition states. Solvent effects (DMSO) were included via SMD model in single-point energy calculations to obtain thermodynamic parameters at the same level of theory. Relative free energies are given in kcal/mol.

In contrast, the more pronounced structural reorganization and highly exergonic nature of the **1a•** formation underscore its greater thermodynamic stability and reinforce the viability of a SET-mediated C–Cl bond activation pathway. Further, **1a•** undergoes radical addition to styrene **3a** to form intermediate **E** through a moderate energy barrier of 8.87 kcal/mol (**TS2**, -62.69 kcal/mol). The consequent radical– radical coupling between **D** and **E** occurs via **TS3** (–80.50 kcal/mol), resulting in the formation of intermediate **F**. Finally, elimination of carbene species occurs through **TS4** (-87.76 kcal/mol), furnishing the desired three-component radical coupling product **4a**, and regenerating the active carbene catalyst. Overall, the entire reaction pathway features favorable energetics with moderate activation barriers and highly exergonic steps, indicating a

Figure 1. Optimized geometry of biaryl radicals.

Journal Name

ARTICLE
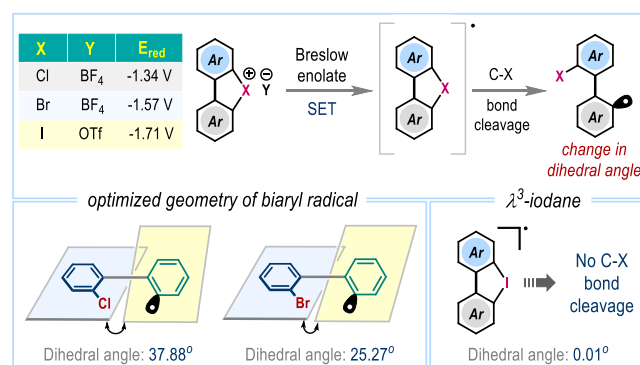
kinetically viable and thermodynamically favorable multistep transformation consistent with the proposed experimental observations. Additionally, we examined a potential radical-mediated two-component coupling involving direct interaction between radical species **D** and radical intermediate **1a•**, occurring prior to the addition of olefin **3a** (grey color). This competing pathway proceeds via transition states **TS2'** (−47.63 kcal/mol) and **TS3'** (−75.54 kcal/mol) to form the two-component product **13**. However, the relatively high activation barrier associated with **TS2'** (23.93 kcal/mol), suggest that the formation of **13** is highly unfavourable under standard reaction conditions. In contrast, the radical addition of **1a•** to styrene **3a** proceeds with a significantly lower barrier of 8.87 kcal/mol, rendering it as the kinetically preferred pathway.

Conclusions

In summary, we have showcased for the first time the radical reaction modality of cyclic diaryl λ^3-chloranes through the development of radical NHC catalysis. The protocol facilitates regioselective olefin difunctionalization in a three-component fashion involving cyclic diaryl λ^3-chloranes, aromatic aldehydes, and olefins in the presence of an NHC-catalyst and offers a diverse range of unsymmetrical 2,2'-biaryls in high yields at room temperature. This aroylarylation protocol is operationally simple, scalable, features a wide substrate generality, and also remains effective in the presence of various medicinally relevant scaffolds. The biaryl products were further diversified via cross-coupling reactions and utilized in Isoxazole synthesis, introducing additional molecular complexity. DFT studies reveal that the pivotal SET process from the Breslow enolate intermediate to the cyclic diaryl λ^3-chlorane is a barrierless process, which is markedly distinct from the corresponding diaryl λ^3-bromane and λ^3-iodane congeners. Further, the lower kinetic barriers associated with the radical relay process and the thermodynamic stability of the product jointly drive the reaction in its desired pathway, overcoming competitive two-component couplings. Notably, this work represents a pioneering advance in the use of λ^3-chloranes in radical NHC catalysis and lays the groundwork for further exploration of their radical chemistry.

Author Contributions

The manuscript was written through contributions of all authors. All authors have given approval to the final version of the manuscript. M. B. and A. A. K have conceptualized the idea. A. A. K., K. P. and M. G. carried out the experiments and mechanistic investigations, and analyzed experimental data. K. L. S. and V. S. K. C. conducted the computational studies. All the authors discussed the results and co-wrote the manuscript.

Conflicts of interest

There are no conflicts to declare.

Data availability

General information, experimental procedures, characterization data for all new compounds, NMR spectra and details of DFT studies are available in the ESI.† Data for the crystal structure reported in this paper have been deposited at the Cambridge Crystallographic Data Centre (CCDC) under the deposition numbers as CCDC 2441452 and CCDC 2444263.

Acknowledgements

Notes and references

1   For a book, see: (a) B. Olofsson, I. Marek and Z. Rappoport, *The Chemistry of Hypervalent Halogen Compounds*, Wiley, 2019, p. 1072; for selected reviews, see; (b) V. V. Zhdankin and P. J. Stang*, Chem. Rev.,* 2008, **108**, 5299–5358; (c) A. Yoshimura and V. V. Zhdankin, *Chem. Rev.,* 2016, **116**, 3328–3435; (d) B. Winterson, T. Patra and T. Wirth, *Synthesis*, 2022, **54**, 1261–1271.

2   For a book, see: (a) V. V. Zhdankin, *Hypervalent Iodine Chemistry: Preparation, Structure and Synthetic Applications of Polyvalent Iodine Compounds*, Wiley, 2013, p. 468; For selected reviews, see; (b) E. A. Merritt and B. Olofsson*, Angew. Chem., Int. Ed.,* 2009, **48**, 9052–9070; (c) L. F. Silva and B. Olofsson, *Nat. Prod. Rep*., 2011, **28**, 1722–1754; (d) X. Wang and A. Studer*, Acc. Chem. Res.,* 2017, **50**, 1712–1724; (e) F. V. Singh, S. E. Shetgaonkar, M. Krishnan and T. Wirth, *Chem. Soc. Rev.*, 2022, **51**, 8102–8139; For selected examples, see: (f) U. Farooq, A. U. H. A. Shah and T. Wirth*, Angew. Chem., Int. Ed*., 2009, **48**, 1018–1020; (g) E. Stridfeldt, E. Lindstedt, M. Reitti, J. Blid, P. O. Norrby and B. Olofsson, *Chem. Eur. J.,* 2017, **23**, 13249–13258; (h) K. Muñiz, *Acc. Chem. Res*., 2018, **51**, 1507–1519; (i) M. Hori, J. D. Guo, T. Yanagi, K. Nogi, T. Sasamori and H. Yorimitsu, *Angew. Chem., Int. Ed*., 2018, **57**, 4663–4667; (j) R. J. Mayer, A. R. Ofial, H. Mayr and C. Y. Legault*, J. Am. Chem. Soc*., 2020, **142**, 5221–5233; (k) G. M. Kiefl and T. Gulder, *J. Am. Chem. Soc.*, 2020, **142**, 20577–20582; (l) K. Miyamoto, M. Saito, S. Tsuji, T. Takagi, M. Shiro, M. Uchiyama and M. Ochiai, *J. Am. Chem. Soc.,* 2021, **143**, 9327–9331; (m) M. Kretzschmar and T. Gulder, *Synlett*, 2023, **34**, 405–413.

3   For a review, see: (a) X. Peng, A. Rahim, W. Peng, F. Jiang, Z. Gu, S. Wen, *Chem. Rev.*, 2023, **123**, 1364–1416; For selected examples, see: (b) R. B. Sandin and A. S. Hay, *J. Am. Chem. Soc.*, 1952, **74**, 274–275; (c) A. Ozanne-Beaudenon and S. Quideau, *Angew. Chem., Int. Ed.*, 2005, **44**, 7065–7069; (d) T. Dohi, M. Ito, N. Yamaoka, K. Morimoto, H. Fujioka and Y. Kita, *Angew. Chem., Int. Ed*., 2010, **49**, 3334–3337; (e) A. H. Sandtorv and D. R. Stuart, *Angew. Chem., Int. Ed*., 2016, **55**, 15812–15815; (f) M. Lanzi, Q. Dherbassy and J. Wencel-Delord, *Angew. Chem.,*

Int. Ed., 2021, **60**, 14852–14857; (g) M. Lanzi, R. A. Ali Abdine, M. De Abreu and J. Wencel-Delord, *Org. Lett.*, 2021, **23**, 9047–9052; (h) D. Carter Martos, M. de Abreu, P. Hauk, P. Fackler and J. Wencel-Delord, *Chem. Sci.,* 2024, **15**, 6770–6776; (i) M. De Abreu, T. Rogge, M. Lanzi, T. J. Saiegh, K. N. Houk and J. Wencel-Delord, *Angew. Chem., Int. Ed.*, 2024, **63**, e202319960.

4   (a) M. Nakajima, K. Miyamoto, K. Hirano and M. Uchiyama*, J. Am. Chem. Soc.*, 2019, **141**, 6499–6503; (b) Y. Watanabe, T. Takagi, K. Miyamoto, J. Kanazawa and M. Uchiyama, *Org. Lett.*, 2020, **22**, 3469–3473; (c) K. Miyamoto and M. Uchiyama, *Chem. Lett.,* 2021, **50**, 832–838; (d) S. S. Karandikar, A. Bhattacharjee, B. E. Metze, N. Javaly, E. J. Valente, T. M. McCormick and D. R. Stuart, *Chem. Sci.,* 2022, **13**, 6352–6540; (e) M. Lanzi and J. Wencel-Delord, *Chem. Sci.*, 2024, **15**, 1557–1569.

5   (a) M. Lanzi, T. Rogge, T. S. Truong, K. N. Houk and J. Wencel-Delord, *J. Am. Chem. Soc.*, 2023, **145**, 345–358; (b) I. O. Putnin, A. A. Sysoeva, M. Il, V and D. S. Bolotin, *ChemCatChem.,* 2024, **16**, e202400672; (c) B. Kang, W. Li, H. Jiang and C. Qi, *Chem. Commun.*, 2025, **61**, 3395–3398; (d) J. Shou and F. Qing, *Org. Lett.*, 2025, **27**, 2815–2820; (e) B. Kang, L. Wei, H. Jiang and C. Qi, *Org. Lett.*, 2025, **27**, 3655–3660; (f) Y. V Safinskaya, M. V Il'in, A. S. Novikov, A. A. Sysoeva and D. S. Bolotin, *J. Org. Chem.*, 2025, **90**, 12080–12087.

6   K. Patra, M. P. Dey and M. Baidya, *Chem. Sci.*, 2024, **15**, 16605-16611.

7   D. Bhattacherjee, B. M. Kariuki, B. A. Piscelli, R. A. Cormanich, and T. Wirth, *Angew. Chem., Int. Ed.*, 2025, *e202424559*.

8   For selected reviews, see; (a) M. Szostak, N. J. Fazakerley, D. Parmar and D. J. Procter, *Chem. Rev.*, 2014, **114**, 5959–6039; (b) Q. Xia, J. Dong, H. Song and Q. Wang*, Chem. Eur. J.*, 2019, **25**, 2949–2961; (c) A. Pe´ter, S. Agasti, O. Knowles, E. Pye and D. J. Procter, *Chem. Soc. Rev.*, 2021, **50**, 5349–5365; (d) Y. Gao and D. Ma, *Nat. Synth.*, 2022, **1**, 275–288.

9   For selected reviews, see; (a) T. Ishii, K. Nagao and H. Ohmiya, *Chem. Sci.*, 2020, **11**, 5630–5636; (b) K-Q. Chen, H. Sheng, Q. Liu, P.L. Shao and X. Y. Chen, *Sci. china Chem.*, 2021, **64**, 7–16; (c) K. Liu, M. Schwenzer and A. Studer, *ACS Catal.,* 2022, **12**, 11984–11999. (d) X. Wang, S. Wu, R. Yang, H. Song, Y. Liu and Q. Wang, *Chem. Sci.,* 2023, **14**, 13367–13383; (e) S. Chakraborty, S. Barik and A. T. Biju, *Chem. Soc. Rev.*, 2024, **54**, 1102–1124.

10   (a) I. Nakanishi, S. Itoh, T. Suenobu and S. Fukuzumi*, Angew. Chem., Int. Ed.*, 1998, **37**, 992–994; (b) I. Nakanishi, S. Itoh and S. Fukuzumi, *Chem. Eur. J.*, 1999, **5**, 2810–2818; (c) L. Delfau, S. Nichilo, F. Molton, J. Broggi, E. Tomàs-Mendivil and D. Martin, *Angew. Chem., Int. Ed.,* 2021, **60**, 26783–26789.

11   For selected reviews, see; (a) H. Ohmiya*, ACS Catal.*, 2020, **10**, 6862–6869; (b) Q. Liu and X-Y. Chen, *Org. Chem. Front.*, 2020, **7**, 2082–2087; (c) J. Liu, X.-N. Xing, J.-H. Huang, L.-Q. Lu and W.-J. Xiao, *Chem. Sci.*, 2020, **11**, 10605–10613; (d) L. Dai and S. Ye, *Chin. Chem. Lett.*, 2021, **32**, 660–667; (e) Q.-Z. Li, R. Zeng, B. Han and J.-L. Li, *Chem. Eur. J.*, 2021, **27**, 3238–3250; (f) P. Bellotti, M. Koy, M. N. Hopkinson and F. Glorius, *Nat. Rev. Chem.*, 2021, **5**, 711–725; (g) A. V. Bay, K. A. Scheidt, *Trends chem.*, 2022, **4**, 277-290; (h) B. Zhang, G. Yang, D. Guo and J. Wang, *Org. Chem. Front.*, 2022, **9**, 5016–5040; (i) Q. Tang, D. Du and J. Gao, *Chem. Eur. J.*, 2023, **26**, e202300832; (j) H. Cai, X. Yang, S. C. Ren and Y. R. Chi, *ACS Catal.*, 2024, **14**, 8270–8293; (j) F. Lu, F. Su, S. Pan, X. Wu, X. Wu and Y. R. Chi, *Chem. Eur. J.*, 2024, **30**, e202401811; For selected examples, see; (l) T. Ishii, Y. Kakeno, K. Nagao and H. Ohmiya, *J. Am. Chem. Soc.*, 2019, **141**, 3854–3858; (m) T. Ishii, K. Ota, K. Nagao and H. Ohmiya, *J. Am. Chem. Soc.*, 2019, **141**, 14073–14077; (n) I. Kim, H. Im, H. Lee and S. Hong, *Chem. Sci.*, 2020, **11**, 3192–3197; (o) K. Ota, K. Nagao and H. Ohmiya, *Org. Lett.*, 2020, **22**, 3922–3925; (p) Y. Kakeno, M. Kusakabe, K. Nagao and H. Ohmiya, *ACS Catal.*, 2020, **10**, 8524–8529; (q) Y. Matsuki, N. Ohnishi, Y. Kakeno, S. Takemoto, T. Ishii, K. Nagao and H. Ohmiya*, Nat. Commun.,* 2021, **12**, 3848; (r) W. Liu, A. Vianna, M. Melaimi, G. Bertrand, X. Yan, W. Liu, A. Vianna, Z. Zhang, S. Huang, L. Huang and M. Melaimi, *Chem Catal.*, 2021, **1**, 196–206; (s) W. D. Liu, W. Lee, H. Shu, C. Xiao, H. Xu, X. Chen, K. N. Houk and J. Zhao, *J. Am. Chem. Soc.*, 2022, **144**, 22767–22777; (t) N. Tanaka, J. L. Zhu, O. L. Valencia, C. R. Schull and K. A. Scheidt, *J. Am. Chem. Soc.*, 2023, **145**, 24486–24492; (u) S. Byun, M. U. Hwang, H. R. Wise, A. V. Bay, P. H. Y. Cheong and K. A. Scheidt, *Angew. Chem., Int. Ed.*, 2023, **62**, e202312829; (v) S. Jana and N. Cramer*, J. Am. Chem. Soc.*, 2024, **146**, 35199–35207; (w) C. Xiao, J.-R. Shan, W.-D. Liu, X. Gao, J. Dai, Z. Wang, W. Wang, K. N. Houk and J. Zhao, *Angew. Chem., Int. Ed.*, 2025, **64**, e202416781 and references therein.

12   Y. H. Liu and D. F. Perepichka, *J. Mater. Chem. C.*, 2021, **9**, 12448–12461.

13   X. Zhu, Y.-F. Wang, W. Ren, F.-L. Zhang and S. Chiba, *Org. Lett.*, 2013, **15**, 3214–3217.

Data Availability Statement

General information, experimental procedures, characterization data for all new compounds, NMR spectra and details of DFT studies are available in the ESI. Data for the crystal structure reported in this paper have been deposited at the Cambridge Crystallographic Data Centre (CCDC) under the deposition numbers are CCDC 2441452 and CCDC 2444263.